Optimal control of an epidemiological Covid-19 model with state constraint

Manuscript submitted to AIMS Journal

doi:10.3934/xx.xxxxxxx

OPTIMAL CONTROL OF AN EPIDEMIOLOGICAL COVID-19 MODEL WITH STATE CONSTRAINT

Elisa Paparelli[✉*1] and Roberto Giambó[✉2,3] and Helmut Maurer [✉4]

[1]Department of Mathematical Sciences "G. L. Lagrange", Dipartimento di Eccellenza 2018-2022, Italy

[2] Mathematics Division, School of Science and Technology, University of Camerino, Italy

[3] INFN, Sezione di Perugia, Italy

[4] Universität Münster, Institut für Analysis und Numerik, Münster, Germany

(Communicated by Handling Editor)

Abstract. The outbreak of the Covid-19 pandemic has forced governments to impose restrictions on the individual liberty of people. Such containment measures have considerably reduced the number of infections but have also caused substantial damage. In this context the following main issue arises: which policy is the best to contain fatalities and economic losses complying with the intensive care units capacity? This issue is investigated through the study of an optimal control problem based on a SEAIRD epidemic model referring to Covid-19. A state constraint is imposed on the number of infected individuals in order to maintain the infectious level under the health-facilities capacity threshold. The challenge is to find a control function that minimizes the total cost which represents a trade-off between economic losses and human deaths. After showing the existence of an optimal solution, the necessary optimality conditions provided by Pontryagin Minimum Principle are derived. Numerical solutions are obtained by discretizing the optimal control problem and applying nonlinear optimization methods. Various scenarios with different initial conditions representing different degrees of infection are studied and the solutions are compared.The COVID-19 control problem treated here may also serve as a prototypical example for solving an epidemiological control model with state constraints.

1. **Introduction.** From December 2019 on, the Covid-19 virus has begun to spread from Wuhan, China [68], hitting later all over the world. In particular, after China, Italy was one of the most affected country, where the outbreak was recorded on February 2020 [54]. Because of this world-wide and rapid spread, on March 11, 2020, the World Health Organization (WHO) declared the COVID-19 outbreak a global pandemic [61]. Nowadays, it still causes many infected people and deaths and thus represents an emergency framework where a large number of aspects are involved. Indeed, not only it provides a health problem, but it has brought to light many issues dealing with economy, sociology and constitutional human rights. The multifaceted complexity of the Covid-19 crisis, makes it a very challenging emergency to be faced

2020 *Mathematics Subject Classification.* Primary: 49N90, 49K15,49M37; Secondary: 91-08.

Key words and phrases. Compartmental epidemiological model, COVID-19, optimal control under state constraint, ICU capacity, non-pharmaceutical interventions.

The first author is supported by [insert grant information here].

*Corresponding author: Elisa Paparelli.

and overcome. It needs ongoing and updated research from biological and medical points of view, starting from genetics, pathogenicity, immunology, epidemiology, etiology and disease treatments.

Many non-pharmaceutical interventions like social distancing, school closure, workplace distancing, restricted public gathering and travel, voluntary case isolation, voluntary quarantine and infection control measures (hand hygiene, cough etiquette, and mask usage) were effective [22, 53]. But in the meantime, many collateral social problems due to social restrictions were involved and increased: domestic violence [48, 16] long-term effects in physical activity and sleep [44], mental illness [62, 65], eating disorders [17], delay in diagnosis as in cancer [38].

Although it has been quantified how containment measures have had a large effects on reducing transmission [18, 29], it has been also questioned how economics was affected by social limitations. The change of people mobility led to dramatic consequences in economics. Indeed it affected the costumer's behavior, ethical issues, business action and aspects related to employees and leadership. Economics consequences evolved and were differentiated in different sectors like tourism, retail, research and education [42]. In addition to these issues, economic implications have tightened the economic gap among people leading to social hardships [9]. At the end, in addition to health emergency, economics and social problems provided important and deep issues that demand attention from governments.

In order to model an epidemic framework and predict its spread, many different approaches are established. For example deterministic compartmental models, stochastic models [3] and epidemic models in complex network [49] have been largely studied. The origins of deterministic epidemiological modeling trace back to the 20th century, experiencing exponential growth from the middle of the 20th century until a tremendous variety of models have now been formulated, mathematically analyzed, and applied to infectious diseases. The mathematical model usually provides a system of differential equations. Many deterministic compartmental models based on the idea of dividing the whole population in compartments as in SIR models, are largely discussed in [26]. Indeed, the introduction of additional compartments allows researchers to study more deeply the dynamic mechanism of Covid-19. For example in [50] susceptible people and susceptible people which are most afraid are distinguished because of their different rate of transmission; in [33] unreported asymptomatic infectious people are taken into account; different levels of being infectious are considered in [45]. In SIDARTHE model the population are divided in eight stages of infectivity: susceptible (S), infected (I), diagnosed (D), ailing (A), recognized (R), threatened (T), healed (H) and extinct (E) [23]. In [64] also vaccinated people are included and in [35] quarantined people. In order to predict the spread of an epidemic related to social closure, in [21] the effect of closure of school looking for the transmission rate between scholar and its effect on the whole population, has been studied.

Optimal control theory [52] is a powerful and successful tool in many fields like aerospace engineering, finance, biology and epidemics. Many applications in biology as in cancer treatment are developed [30]. In infectious disease it provides the best interventions strategies to flatten the curve of infectivity. For example one can minimize the number of infections, the cost of the control, or both [60]. Many studies are focused on vaccination policies where the aim is to minimize the vaccination cost [46] or the sum of vaccination and infected people, with a threshold constraint on vaccinated population [8], and in multi objective framework [31].

Other approaches aimed to find optimal allocation strategy in vaccination in order to minimize deaths. The optimal vaccine allocation in different age-groups is investigated [39]. Many studies investigate the optimal policy where controls are provided by the level of hospitalization and quarantine [63], personal protections and contact-tracing (diagnoses) [4, 13] and the objective included a theoretical economic cost of implementing two controls. Other different objectives and controls in infectious diseases are largely discussed in [7, 58, 43, 1, 51, 69, 2, 34, 57, 10, 32]. Also the control on people awareness due to media coverage and the control that minimizes the total treatment cost, is investigated [36]. In [55] and [24] the optimal control is constrained to an age-structured model.

Some studies, that consider intensive care units (ICU) included in the optimal control formulation, are of interest to us. In [41] the control must be as close as possible to a certain transmission rate to avoid overloading of the ICU capacity. The pandemic emergency led governments to impose non-pharmaceutical interventions, especially in social restrictions, that caused significant economic losses all over in the world. Compared to previous work, our aim is to include the economic cost that tries to fit the real-world phenomena of economic losses due to social restrictions.

In studies that detected the tradeoff between infectivity and economic losses, the cost is linear [14] or quadratic [12] with respect to the control function. Kantner and Koprucki [27] proposed a different objective to be minimized: on the one hand, the number of disease-related deaths are minimized by strictly avoiding an overcrowd of the intensive care treatment capacities, on the other hand sufficient immunity must be established in the population in the long run to prevent a second outbreak of the epidemic. The aim of this work is the investigation of an optimal control that provides a trade-off between human deaths and economic losses by improving non-pharmaceutical interventions as social restrictions and personal control measures. We exclude the possibility of complete eradication and vaccination. Additionally, we want to include the threshold of ICU capacity in order to avoid the overcrowding of national health systems as an additional state constraint in the formulation of the problem. Indeed, our aim is to look for the best policy that flattens the curve, balances deaths and economics and at the same time satisfies the health system capability. Our starting point is the model developed by Aspri et al. [5]. They extend the classical SIR compartmental model to a SEAIRD model and introduce a realistic cost functional related to control policy, where the economic losses were well-modeled taking into account gross domestic production losses due to Covid-19 restrictions. The cost functional is convex with respect to the control but is neither quadratic nor linear, as commonly considered in literature. In addition to this, they measure a statistical value of life that represents the fraction of GDP related welfare that the social planner is willing to renounce to save an actualized 1 % of Covid mortality. The type of cost functional proposed by [5] implies that the strict Legendre-Clebsch condition holds. It then follows from the Pontryagin Minimum Principle that the optimal control is a *continuous* function. It provides the best level of control at each time, but this type of control represents an *idealized policy* since its continuity cannot be really implemented by governments. However, the optimal continuous control can be conveniently approximated by a control that is piecewise constant on a given segmentation of the planning interval. This will be demonstrated in Section 5.3.4 on one instance for the large terminal time $T = 200$.

In section 2 we discuss the dynamic features of the SEAIRD model for COVID-19. Section 3 introduces the cost functional and presents the optimal control problem.

Moreover, an upper bound for the number of infected people is imposed as a state constraint. It is shown that an optimal solution to the optimal control exists. In Section 4 we evaluate the necessary optimality conditions for the state-constrained optimal control problem. Since the state constraint satisfies a regularity condition, we can use the direct adjoining approach in Pontryagin's Minimum Principle as discussed in [25]. Section 5 presents the optimal control and the state trajectories for three scenarios corresponding to different initial conditions and terminal times. The results are obtained by applying either boundary value methods associated with the Maximum Principle or by discretization and nonlinear programming methods. The state-constrained solutions are compared to the solutions without the state constraint.

2. **Controlled Epidemiological Model for Covid-19.** We introduce an optimal control problem for an epidemiological model of Covid-19 starting from the formulation in Aspri, Gandolfi et al [5]. The underlying dynamics is a compartmental epidemic model based on the classical SIR model which is adapted to epidemiological features of Covid-19 using current observations. The population is divided into compartments defining the following state variables: susceptible (S), exposed (E), asymptomatic (A), infected with symptoms (I), recovered (R), Covid related deceased (D) and natural deaths (D_N). These variables are functions of time t, but in the sequel we omit the t-dependence in our notation for better readability. The state variables are normalized so that

$$S + E + A + I + R + D = 1, \tag{1}$$

A natural death rate n is considered and an equal natural birth rate compensates it. The birth rate can be seen as the rate of new "labor force", with a little bit of linguistic abuse, to be included in the compartments. It is reduced because of the Covid death compartment that does not contribute to new birth. The dynamic model is the following:

$$\text{Susceptible} \quad \dot{S}(t) = -\beta u S(sI + E + A) - nS + n(1 - D) \tag{2}$$

$$\text{Exposed} \quad \dot{E}(t) = \beta u S(sI + E + A) - (k + n)E \tag{3}$$

$$\text{Asymptomatic} \quad \dot{A}(t) = (1 - \epsilon)kE - (\gamma + n)A \tag{4}$$

$$\text{Infected} \quad \dot{I}(t) = \epsilon kE - (\gamma + \delta + n)I \tag{5}$$

$$\text{Recovered} \quad \dot{R}(t) = \gamma(A + I) - nR \tag{6}$$

$$\text{Covid deceased} \quad \dot{D}(t) = \delta I \tag{7}$$

$$\text{Natural deaths} \quad \dot{D_N}(t) = n(S + E + A + I + R) \tag{8}$$

The initial population at the onset of the outbreak consists of only susceptibles, $S(0) \approx 1$ and a small fraction of exposed such that $S(0) + E(0) = 1$:

$$S(0) = 1 - E(0), \quad E(0) = 10^{-6}, \quad A(0) = I(0) = R(0) = D(0) = 0. \tag{9}$$

We point out that the normalization (1) is consistent with the initial condition (9) and equations (2)-(7), since they imply $d/dt(S + E + A + I + R + D) = 0$. We refer to [5] the discussion about epidemic modeling and all details of the choice of parameters reported in table 1. The probability of a susceptible individual to come in contact with an asymptomatic person and an exposed one is the same, while the probability to have contact with an infected individual is reduced by a factor $s < 1$. This parameter can be seen as the result of isolation measure after the positivity

test; it is independent of the government restrictions which justifies the presence of this parameter. Notice that compared to the model proposed by Aspri et al. [5] we do not reduce the transmissibility of population E and A. The rate β represents the transmission of the virus, and it is mitigated by the factor $u(t)$ which represents the control variable. It represents the external action to reduce the spread of the epidemic, modulating the interactions between susceptible individuals and either exposed, asymptomatic or infected people. This is a crucial point of our model: we act only in this term trough the control function $u(t)$, modifying the transmissibility. The control $u(t)$ satisfies the control constraint

$$0 < u_0 \leq u(t) \leq 1 \text{ for a.e } t \in [0, T], \tag{10}$$

for a finite time horizon $T > 0$. When the control is at its upper bound $u(t) = 1$, then there are no lockdown restrictions. The lower bound u_0 corresponds to the infeasibility of a complete shutdown, since there will always be a minimum of interactions and economic productivity. From a realistic point of view, it is not possible to totally isolate individuals from each other and interrupt every kind of activity as, for example, through home production with smart working. Gandolfi et al. [5] assumed that the control is a continuous, piece-wise linear function, with the additional constraint of being constant for long enough time intervals. In contrast with this assumption we impose that the control $u(\cdot)$ is a measurable and essentially bounded function:

$$u \in L^\infty([0, T], \mathbb{R}).$$

Thus, the admissible control set in function space is given by

$$U_{ad} = \{u \in L^\infty([0, T], \mathbb{R}) \,|\, u_0 \leq u(t) \leq 1 \text{ for a.e } t \in [0, T]\}. \tag{11}$$

We denote the state vector of the dynamic system (2)-(7) by

$$X := (S, E, A, I, R, D) \in \mathbb{R}^6.$$

Let $u \in U_{ad}$ be an admissible control and let $X(t)$ be a solution to (2)-(7) and (9) in the time interval $[0, T]$. The next lemma establishes the non-negativity and boundedness of the solution.

Lemma 2.1. *The solution satisfies the following componentwise estimates*

$$0 \leq S(t), E(t), A(t), I(t), R(t), D(t) \leq 1 \quad \forall\, t \in [0, T].$$

Proof. The essential elements of the proof proceed by contradiction. We begin with showing the non-negativity of the solution. Consider the variable $S(t)$ for which we will show that $S(t) > 0$ holds in $[0, T]$. Since $S(0) > 0$ we have $S(t) > 0$ for $0 \leq t \leq c$ with $c > 0$. Suppose that $t_0 > 0$ were the first time with $S(t_0) = 0$. From (2) we get $\dot{S}(t_0) = n(1 - D(t_0)) \geq 0$. Indeed, assume on the contrary that $D(t_0) > 1$. This would imply that at least one of the variables S, E, A, I, R vanishes at a time $t < t_0$. But we assumed that t_0 is the first time with $S(t_0) = 0$. Hence we have $S(\tilde{t}) > 0$. The proof that the other variables E, A, I, R cannot vanish follows from the arguments below. In the case $D(t_0) = 1$ we would get $S(t_0) = E(t_0) = A(t_0) = I(t_0) = R(t_0) = 0$ and, hence, the solution is identically zero, which contradicts the initial condition (9). Then equation (2) gives $\dot{S}(t_0) > 0$ and, hence, $S(t)$ is strictly increasing at t_0, which is a contradiction. From an analogous argument we can conclude that $S(t)$ can not approach 0 so that we can fix a sufficiently small $c > 0$ such that $S(t) \geq c$ for all $t \in [0, T]$.

Consider now the solutions $E(t), A(t), I(t)$. Since $E(0) > 0$ and $A(0) = R(0) = I(0) = 0$ we have $E(t) > 0$ in a right neighborhood of $t = 0$. Moreover, $\dot{A}(0) > 0$, resp., $\dot{I}(0) > 0$ imply that $A(t) > 0$, resp., $I(t) > 0$ holds in a right neighborhood of $t = 0$. The second derivative of R is obtained from (4)-(6) as $\ddot{R}(0) = k\gamma E(0) > 0$ which yields $R(t) > 0$ in a right neighborhood of $t = 0$. So far, we have shown that $E(t), A(t), I(t), R(t) > 0$ in a right neighborhood of $t = 0$.

Suppose now that one of variables E, A, I, R vanishes at a time $t_0 > 0$. Assume A to be the first variable with $A(t_0) = 0$. Since it is not be possible that $A(t)$ is strictly increasing at $t = t_0$, this implies $\dot{A}(t_0) = 0$ and thus $E(t_0) = 0$. The second derivative of A is given by

$$\ddot{A}(t_0) = (1-\epsilon)k\dot{E}(t_0) = (1-\epsilon)k\beta u(t_0)S(t_0)sI(t_0) > 0$$

which implies that $A(t)$ has a minimum at t_0 and, as a consequence, will not become negative. Similarly, one can show $I(t) \geq 0$ and $R(t) \geq 0$.

If $E(t)$ would vanish first at $t = t_0$, we necessarily would have $\dot{E}(t_0) = 0$, since $E(t)$ cannot increase at t_0. Then from equation (3) we obtain $A(t_0) = I(t_0) = 0$. Taking the initial condition $(S_0, 0, 0, 0, R_0, D_0)$ in $t = t_0$, the solution of (2)–(7) is given by

$$R(t) = R_0 e^{-n(t-t_0)}, \quad D(t) \equiv D_0, \quad S(t) = 1 - D(t) - R(t).$$

Hence, we can conclude that the state variables E, A, I, R cannot become negative.

To show the boundedness of the solution we consider the sum $W := S + E + A + I + R + D$ of state variables. The derivative of $W(t)$ is readily computed using the equations (2)–(7) as $\dot{W}(t) = n(1 - W(t))$. Since $W(0) = 1$ in view of the initial conditions (9), it follows that $W(t) \equiv 1$. Then the non-negativity of the variables yields the componentwise bound $S(t), E(t), A(t), I(t), R(t), D(t) \leq 1$ for all $t \in [0, T]$. □

3. **Cost functional and optimal control problem for Covid-19.** The aim of this work is to determine the best control that mitigates the virus spread, but balances the effect of overall deaths and losses of "production". From now on, with a little bit of linguistic abuse, we call production what concerns the creation of money and generates economic strength in the community. Hence, the social planner has to minimize a functional F that combines production P and the number of new deaths due to Covid $\dot{D}(t) = \delta I(t)$, (7). The functional is formulated starting from the form

$$F = \int_0^T e^{-rt}[\mathcal{V}(P) + a\dot{D}]dt, \tag{12}$$

where T is fixed. The presence of the exponential factor represents the discount factor that actualizes cost, where r is the discounting rate. As a consequence, it incorporates the lesser interest for more distant economic consequences and the preference for the present cases of death. Hence it acts in the direction of flattening the infection curve. The function $\mathcal{V}(P(t))$ is a decreasing convex function that expressed the loss of the GDP related to the production $P(t)$, defined as

$$\mathcal{V} = -\frac{P^{1-\sigma} - 1}{1 - \sigma}, \tag{13}$$

where $\sigma > 1$, indeed for the productivity at maximum level, i.e $P = 1$, there is no loss. We express P as a function on population that actively contribute on

variation in gross domestic production, through economic consumption and through the workforce, i.e. S, E, A and R, as

$$P(u, X) = u^{\theta}(S + E + A + R), \tag{14}$$

with $\theta \in (0, 1)$, that relates the effect of social restrictions on economical activities. We point out the fact that as with all compartmental models, it is assumed that each compartment is homogeneous, meaning each individual within the same compartment is indistinguishable from the others. This inevitably leads to an inability to distinguish individuals of different ages, that contribute differently on economic consequences. Recalling the state $X = (S, E, A, I, R, D) \in \mathbb{R}^6$, the cost functional is finally modeled as follows:

$$F(X, u) = \int_0^T e^{-rt} \left[- \frac{(u^{\theta}[S + E + A + R])^{1-\sigma} - 1}{1 - \sigma} + a\dot{D} \right] dt. \tag{15}$$

The estimation of parameter a is particularly complicated. Since it represents the social cost of a Covid death, thus it translates the human life as a life cost in economic term, it depends on socio-political and economic factors that vary from country to country. About what concerns the parameters σ and θ, they are estimated from data referred to some western countries such as France, Germany, Italy and US, to be respectively, 2 and 1/3. We refer the reader to [5] for every details concerning economical arguments on the above parameters estimation. Hence, the objective involves the control function term $u^{-1/3}$, that is a new element compared to many works where the cost functionals depend either quadratically or linearly on the control; see, eg., [59]. Besides the control constraint (10) we consider the state constraint

$$I(t) \leq I_{max} \quad \forall\, t \in [0, T]. \tag{16}$$

The aim is to determine a control policy that constrains the trajectory of infected people to a restricted phase region. The threshold I_{max} represents the maximum capacity of a government to manage infected people with health assistance and, for severely ill people, to guarantee intensive care places in hospitals. Many problems in the epidemiological literature consider similar state constraints or mixed control-state constraint [15, 8, 12]. With regard to the threshold value I_{max}, we argue as follows. According to [6] at the first epidemic wave in Europe, 2.4% of infected people needed intensive care and the availability of Intensive Care Units in average was 11.5 per 100000 people. Since we want to avoid infected people $I(t)$ needing ICU which would exceed the maximum capacity of the health care system, we consider the constraint $0.024 \cdot I(t) \leq 115/10^6$ and thus

$$I(t) \leq \frac{115}{10^6 \cdot 0.024} = 4.79 \cdot 10^{-3} \approx 0.005.$$

Hence, we consider the threshold

$$I_{max} = 0.005.$$

The percentage of critical infectious has decreased in the meantime, as it is reported day by day in *worldometers.info* and at the same time governments invested in increasing Intensive Care Units. Despite these facts, we prefer to take into account the first period of virus spread. Since we want to consider a realistic scenario where the restrictions policy presumably would start after the evidence of some infectious cases, our optimal control problem is not complemented by the initial conditions (9) but the dynamics starts from the scenarios of three sets of initial conditions which

are obtained by integrating the dynamics (2)–(7), (9) in absence of any control policy, i.e., $u(t) \equiv 1$, up to times $T_0 = 55, T_0 = 65$ and $T_0 = 70$.

Case 1. Integration of (2)–(7), (9) with $u(t) \equiv 1$ up to time $T_0 = 55$ days.

$$X_0 = [0.9979, 7.713 \cdot 10^{-4}, 1.941 \cdot 10^{-4}, 3.841 \cdot 10^{-4}, 6.463 \cdot 10^{-4}, 8.58904 \cdot 10^{-6}]. \quad (17)$$

Since the number of exposed people is less than 800 in one million people, this scenario indicates a mild spread of the epidemic.

Case 2. Integration of (2)–(7), (9) with $u(t) \equiv 1$ up to time $T_0 = 65$ days.

$$X_0 = [0.9932, 0.002614, 6.601 \cdot 10^{-4}, 0.001306, 0.002208, 2.934 \cdot 10^{-5}]. \quad (18)$$

In this case we there are about 2600 people exposed in one million and, hence, this case can be considered as an advanced epidemic.

Case 3. Integration of (2)–(7), (9) with $u(t) \equiv 1$ up to time $T_0 = 70$ days.

$$X_0 = [0.9873, 0.004853, 0.001229, 0.002434, 0.004138, 5.499 \cdot 10^{-5}]. \quad (19)$$

Since at day $T_0 = 70$ from the first exposure, the exposed class contains almost 5000 in one million people, the virus has severely spread out.

Remark 3.1. In the 3 scenarios of initial conditions (17)-(19) we have $0 < X_i(0) < 1$ for $i = 1, \dots, 6$. Here, we can improve Lemma 2.1 since we get a positive lower bound for the trajectories: there exists $c > 0$ with $c \leq X_i(t)\ \forall\, t \in [0, T]$, $i = 1, \dots, 6$. The positive lower bound follows from the estimates in the proof of Lemma 2.1 and the continuity of the state variables $X_i(t)$.

In summary, the ingredients of our optimal control problem (OCP) for Covid-19 are as follows:

$$\left.\begin{array}{ll} \text{(OCP)} & \text{Minimize}_{\,u \in U_{ad}}\ F(X,u) \quad \text{subject to the dynamical} \\ & \text{equations (2)} - \text{(7)}, \text{ initial conditions (17), (18), (19),} \\ & \text{control constraint (10) and state constraint (16).} \end{array}\right\} \quad (20)$$

where the parameters involved in the model are reported in table (1). Now let us

TABLE 1. Parameter values

Parameter	Value	Definition
β	0.25	The infection rate
s	0.1	Proportion of infected people who develop symptoms
n	0.00003	The natural death rate
k	0.2	The latency period after infection
ϵ	2/3	The fraction of asymptomatic
γ	0.14	The recovery period
δ	0.0028	The death rate due to Covid-19
r	0.04	The economic discount rate
σ	2	A parameter that expresses the GDP losses on production
θ	1/3	Elasticity parameter that expresses the dependence of GDP change on infection spread
a	7833.11	The social cost of human deaths due to Covid-19
I_{max}	0.005	Intensive Care Units availability

write the optimal control problem for Covid-19 in a compact form that allows to

evaluate the necessary optimality conditions in the next section in a more convenient form. Denoting the right hand sides of the ODEs (2)-(7) by $f(X,u)$ we have the dynamic system

$$\dot{X}(t) = f(X(t),u(t)), \quad X(0) = X_0. \tag{21}$$

Introducing the function $h(X) := I - I_{max}$, the state constraint (16) is formally written as

$$h(X(t)) = I(t) - I_{max} \leq 0, \quad \forall t \in [0,T]. \tag{22}$$

The objective functional is given by

$$F(X,u) = \int_0^T e^{-rt} f_0(X(t),u(t))\, dt \tag{23}$$

where

$$f_0(X,u) = \frac{1-(u^\theta[S+E+A+R])^{1-\sigma}}{1-\sigma} + a\delta I. \tag{24}$$

Proposition 3.2. *(Existence of an optimal solution)*
The optimal control problem (OCP) defined in (20) has an optimal solution for terminal times $T \leq 200$.

Proof. We use the existence result in Cesari, [11], p. 314, Theorem 9.3.i. Then we have to verify the following three properties:

(1) The family of admissible controls is not empty.
(2) There exists a uniform bound $||X(t)|| \leq b$ on $[0,T]$ for all responses $X(t)$ to admissible controls.
(3) The extended velocity set
$$V(t,X) = \{\, (e^{-rt} f_0(X,u) + \alpha, f(X,u)) \,|\, \alpha \geq 0, u_0 \leq u \leq 1 \,\}$$
is convex in $\mathbb{R} \times \mathbb{R}^6$ for each fixed (t,X).

To show claim (1), we integrate the system (2)-(7) with initial conditions (17), (18) (19) using the control $u(t) = u_0 = 0.001$ which represents maximal restriction; see Figure 1. For all three scenarios of initial conditions and all terminal times $T \leq 200$ we get the following upper bound for infected individuals (see eg. Figure 1 for $T = 70$):

$$\max\{\, I(t) \,|\, 0 \leq t \leq T \,\} \leq 0.0028 < I_{max} = 0.005.$$

Property (2) follows directly from Lemma 2.1. The convexity property (3) is a consequence of the fact that the control u enters the dynamics linearly and appears as the factor $u^{-1/3}$ in the objective functional, since $\sigma = 2$ and $\theta = 1/3$. We remark that, according to definitions (13)-(14), $\sigma > 1$ and $\theta \in (0,1)$, the control enters as $u^{\theta(1-\sigma)}$ hence the condition still holds true even without fixing their values. □

4. **Pontryagin Minimum Principle: necessary optimality conditions.** We evaluate the necessary optimality conditions in Pontryagin's Minimum Principle for state-constrained optimal control problems which are discussed in Jacobson, Lele, Speyer [28], Maurer [37], Vinter [66] and surveyed in Hartl, Sethi, Thompson [25]. Let us start with some basic notions for the state constraint $I(t) \leq I_{max}$ as adopted from the review [25]. A subinterval $[t_1,t_2] \subset [0,T]$ with $t_1 < t_2$ is called an *interior interval*, if $I(t) < I_{max}$ holds for all $t_1 < t < t_2$. An interval $[t_1,t_2] \subset [0,T]$ with $t_1 < t_2$ is called a *boundary interval*, if $I(t) = I_{max}$ holds for all $t_1 \leq t \leq t_2$. If the interval $[t_1,t_2]$ is maximal with this property, then t_1 is called an *entry-time* and t_2 is called an *exit time*. If $t_s \in [0,T]$ is an isolated time with $I(t_s) = I_{max}$, then t_s is called a *contact time*. Taken together, entry, exit and contact times are called

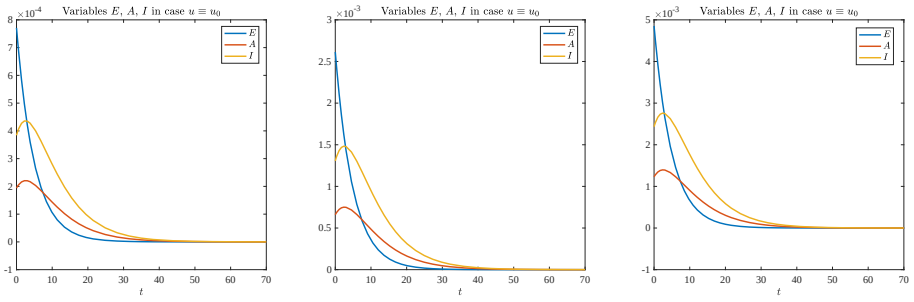

(A) (B) (C)

FIGURE 1. Covid-19 spread under control $u \equiv u_0 = 0.001$, according to equations (2)-(7) for the three initial conditions (17)-(18)-(19).

junction times. The *direct adjoining approach* in [25], [37] requires the *regularity* of the state constraint $h(X(t)) = I(t) - I_{max} \leq 0$ in (22). Since the second total time derivative of $h(X(t))$ is the first derivative that contains the control explicitly, the state constraint has *order two*. Indeed, omitting the explicit time argument we have

$$\frac{d^2}{dt^2}h(X) = \epsilon k\beta u S(sI + E + A) - \epsilon k(k + 2n + \gamma + \delta)E + (\gamma + \delta + n)^2 I. \tag{25}$$

Along any *boundary arc* with $I(t) = I_{max}$ the following regularity condition holds

$$\frac{\partial}{\partial u}\frac{d^2}{dt^2}h(X) = \epsilon k\beta S(sI + E + A) \neq 0. \tag{26}$$

It follows that the *boundary control* is determined by the feedback expression

$$u_b(X) = \frac{\epsilon k(k + 2n + \gamma + \delta)E - (\gamma + \delta + n)^2\, I}{\epsilon k\beta S(sI + E + A)}. \tag{27}$$

The *standard* Hamiltonian is given by

$$H(X, \lambda, u, t) = \lambda_0 e^{-rt} f_0(X, u) + < \lambda, f(X, u) >, \tag{28}$$

where $\lambda = (\lambda_S, \lambda_E, \lambda_A, \lambda_I, \lambda_R, \lambda_D) \in \mathbb{R}^6$ denotes the adjoint variable and $\lambda_0 \geq 0$ is a nonnegative scalar. The regularity condition (26) allows us to use the *direct adjoining approach* where the state constraint is directly adjoined to the Hamiltonian (28) by a scalar multiplier η; see [25], section 4, and [37]. This defines the *augmented* Hamiltonian

$$\mathcal{H}(X, \lambda, \eta, u, t) = \lambda_0 e^{-rt} f_0(X, u) + < \lambda, f(X, u) > +\eta\,(I - I_{max}). \tag{29}$$

To eliminate the discount factor e^{rt} it is convenient to consider the *current-value augmented Hamiltonian*

$$\mathcal{H}^c(X, \lambda, \eta, u) = \lambda_0\, f_0(X, u) + < \lambda, f(X, u) > +\eta\,(I - I_{max}). \tag{30}$$

The adjoint variable λ and the multiplier η for the augmented *current-value* Hamiltonian (30) are related to the adjoint variable $\tilde{\lambda}$ and multiplier $\tilde{\eta}$ of the augmented Hamiltonian (29) by

$$\lambda(t) = e^{rt}\tilde{\lambda}(t), \quad \eta(t) = e^{rt}\tilde{\eta}(t), \tag{31}$$

We obtain necessary optimality conditions for problem (20) by combining the results in Jacobson, Lele and Speyer [28], Maurer [37] and Vinter [66], Chapter 9.3, with the survey in Hartl, Sethi and Vickson [25], Informal Theorem 4.1, Theorem 4.2 and Proposition 4.1. Our notations are a bit different, because the multiplier $\eta(t)$ for the state constraint, which appears in the following theorem, is the density of the function $\mu(\cdot)$ of bounded variation on boundary arcs associated with the state constraint; see [37].

Theorem 4.1. *(Minimum Principle)*
Let $(X^*(\cdot), u^*(\cdot)) \in W^{1,\infty}([0,T],\mathbb{R}^6) \times L^\infty([0,T],\mathbb{R})$ *be an optimal solution of the optimal control problem* (OCP) *in* (20). *Assume that there are only finitely many junction times. Moreover, assume that on every boundary interval* $[t_1,t_2]$ *the boundary control* $u_b(X(t))$ *is in the interior of the control set* $\Omega = [u_0,1]$, *i.e.,* $u_0 < u_b(X(t)) < 1$ *for* $t_1 < t < t_2$. *Then there exist a constant* $\lambda_0 \geq 0$, *a piecewise absolutely continuous adjoint function* $\lambda : [0,T] \to \mathbb{R}^6$, *a piecewise continuous multiplier function* $\eta : [0,T] \to \mathbb{R}$, *multipliers* ν_s *at every junction time* $t_s < T$, *and a multiplier* ν_T *such that* $(\lambda_0, \lambda(t), \eta(t), \nu_1, \nu_2, .., \nu_T) \neq 0 \quad \forall\, t \in [0,T]$ *and the following conditions hold for almost all* $t \in [0,T]$*:*

Minimizing control*:*

$$u^*(t) = arg\,min_{\,u_0 \leq u \leq 1}\, \mathcal{H}^c(X^*(t), \lambda(t), \eta(t), u)\,. \tag{32}$$

Adjoint equations*:*

$$\begin{aligned} \dot\lambda(t) - r\lambda(t) &= -\tfrac{\partial}{\partial X}\mathcal{H}^c(X^*(t), \lambda(t), \eta(t), u^*(t) \\ &= -\lambda_0 \tfrac{\partial}{\partial X} f_0(X^*(t), u^*(t)) - \tfrac{\partial}{\partial X} < \lambda(t), f(X^*(t), u^*(t)) > \\ &\quad -\eta \tfrac{\partial}{\partial X} h(X^*(t))\,. \end{aligned} \tag{33}$$

Transversality condition*:*

$$\lambda_S(T) = \lambda_E(T) = \lambda_A(T) = \lambda_R(T) = \lambda_D(T) = 0,\ \lambda_I(T) = \nu_T\,. \tag{34}$$

Jump condition for adjoint variable λ_I *at a junction time* t_s*:*

$$\lambda(t_s+) = \lambda(t_s-) - \nu_s \frac{\partial h}{\partial X}(X^*(t_s)), \quad i.e., \quad \lambda_I(t_s+) = \lambda_I(t_s-) - \nu_s, \quad \nu_s \geq 0. \tag{35}$$

Complementarity conditions:

$$\eta(t) \geq 0,\ \eta(t)\,(I^*(t) - I_{max}) = 0, \quad \nu_T\,(I^*(T) - I_{max}) = 0. \tag{36}$$

Remark 4.2.

1. If the multiplier $\lambda_0 \geq 0$ is positive, it can be normalized to $\lambda_0 = 1$. The case $\lambda_0 = 0$ is called the *abnormal* case. If the state constraint does not become active, we have a control problem with free terminal state which yields $\lambda(T) = 0$. Then $\lambda_0 = 0$ would immediately lead to $\lambda(t) \equiv 0$ which contradicts the fact that we have a set of nonzero multipliers. For an active state constraint we cannot exclude the *abnormal case* $\lambda_0 = 0$ a priori, but our computations in Section 5 for the three scenarios of initial conditions (17)-(19) yield solutions with $\lambda_0 = 1$.
2. The assumption that the boundary control $u_b(X(t))$ lies in the interior of the control set can not be checked a priori for the control problem (20). But the figures in Section 5 displaying the control $u(t)$ will show that this assumption is satisfied.

In the following, we shall suppress the upper index star denoting the optimal solution. The control u is determined by the minimum condition (32) as a function of the state X and adjoint variable λ in the following way. If $u_0 < u(t) < 1$, the minimum condition (32) yields

$$\begin{aligned} 0 = \mathcal{H}_u^c(X,\lambda,\eta,u_f) &= -\theta u_f^{\theta(1-\sigma)-1}(S+E+A+R)^{(1-\sigma)} - \lambda_S\beta S(sI+E+A) \\ &\quad +\lambda_E\beta S(sI+E+A), \end{aligned}$$

where u_f denotes the so-called free control. This equation yields the following free control with exponent $z = \frac{1}{\theta(1-\sigma)-1}$:

$$u_f(X,\lambda) = \left[-\frac{(S+E+A+R)^{\sigma-1}}{\theta}\left(\lambda_S\beta S(sI+E+A)+\lambda_E\beta S(sI+E+A)\right)\right]^z. \tag{37}$$

Then the optimal control $u(X,\lambda)$ is obtained by projecting the free control $u_f(X,\lambda)$ onto the admissible control set $[u_0,1]$:

$$u(X,\lambda) = \max\{u_0, \min\{1, u_f(X,\lambda)\}\}. \tag{38}$$

Note that the determination of $u_f(X,\lambda)$ from the equation $H_u(X(t),\lambda,u) = 0$ is made possible by the fact that the *strict Legendre-Clebsch condition* holds:

$$\frac{\partial^2\mathcal{H}^c}{\partial u^2} = -\theta(S+E+A+R)^{(1-\sigma)}(\theta(1-\sigma)-1)u^{\theta(1-\sigma)-2} > 0, \tag{39}$$

for every values of σ, θ that are consistent with definition given by (13)-(14), hence it is true for the fixed values $\theta = 1/3$ and $\sigma = 2$. Since the functions $f_0(X,u), f(X,u), h(X)$ are of class C^∞ in appropriate open domains, a formula for the multiplier $\eta(t)$ for the state constraint can be determined recursively; see [37] and [25], Proposition 4.1 and equation (4.22). Moreover, we get the following smoothness properties of the control, adjoint variable and multiplier.

Corollary 4.3. *Under the assumptions in Theorem 4.1 the following continuity and smoothness properties hold.*

(a) The optimal control $u(\cdot)$ is continuous on $[0,T]$ including the junction points.

(b) The optimal control $u(\cdot)$, the adjoint function $\lambda(\cdot)$ and the multiplier $\eta(\cdot)$ are piecewise of class C^∞.

Proof. The continuity of the optimal control $u(\cdot)$ follows from the fact that the strict Legendre-Clebsch condition (39) holds and the Hamiltonian $\mathcal{H}^c$ is *regular*, i.e., has a uniquely defined minimum given in (37) and (38); see [28], [37], Hartl et al. [25], Proposition 4.3. We point out that the strict convexity of the cost integral on u is the key point to assure the continuity. Claim (b) is a consequence of the fact that the functions $f_0(X,u), f(X,u), h(X)$ are of class C^∞ using the formulas for the boundary control (27) and free control (37). □

It is rather tedious to integrate the adjoint equations (33) numerically. Using discretization and nonlinear programming methods, the adjoint variables can be identified by the Lagrange multipliers associated with the discretized differential equations and thus can be recovered from the optimization code. Nevertheless, for the sake of completeness and for using the adjoint equations in boundary value

approaches we give the adjoint equations (33) explicitly:

$$\left.\begin{aligned}
\dot\lambda_S &= r\lambda_S + u^{(1-\sigma)\theta}(S+E+A+R)^{-\sigma} + \lambda_S(n+\beta u(sI+E+A)) \\
&\quad -\lambda_E\beta u(sI+E+A), \\
\dot\lambda_E &= r\lambda_E + u^{(1-\sigma)\theta}(S+E+A+R)^{-\sigma} + \lambda_S\beta uS - \lambda_E(\beta uS-(k+n)) \\
&\quad -\lambda_A(1-\epsilon)k - \lambda_I k\epsilon, \\
\dot\lambda_A &= r\lambda_A + u^{(1-\sigma)\theta}(S+E+A+R)^{-\sigma} + \lambda_S\beta S - \lambda_E\beta uS + \lambda_A(\gamma+n) \\
&\quad -\lambda_R\gamma, \\
\dot\lambda_I &= r\lambda_I - a\delta + \lambda_S\beta suS - \lambda_E\beta suS + \lambda_I(\gamma+\delta+n) - \lambda_R\gamma - \lambda_D\delta - \eta, \\
\dot\lambda_R &= r\lambda_R + u^{(1-\sigma)\theta}(S+E+A+R)^{-\sigma} + \lambda_R n, \\
\dot\lambda_D &= r\lambda_D + \lambda_S n - \lambda_D\delta.
\end{aligned}\right\} \tag{40}$$

Remark 4.4. In summary, the necessary conditions represent a mixed system of differential and algebraic equations. In the absence of the state constraint $I - I_{max} \leq 0$, the dynamic equations (21) and adjoint equations (40) lead to a *boundary value problem* for the variables (X, λ) by inserting the control expression (38):

$$\begin{cases} \dot X(t) = f(X(t), u(X(t), \lambda(t))), & X(0) = X_0 \\ \dot\lambda(t) = g(X(t), \lambda(t)), & \lambda(T) = 0 \end{cases} \tag{41}$$

where $g(X, \lambda)$ denotes the dynamics of adjoint variables (40). Following the approach employed in [20], in this setting and from the estimation bounds of variables, see (3.1), the uniqueness of optimal control for $T > 0$ can be rigorously prove. This setting will be implemented in the next section in order to compare optimal costs and epidemiological scenarios with and without the infected population constraint.

5. **Numerical solutions.** In this section, we present numerical results for the solutions of the optimal control problem (20). We prescribe the three initial conditions (17), (18), (19) representing a mild, intermediate and severe epidemic scenario and compute solutions for a small and a much larger terminal time T. In each case, we compare the solutions of the problem (20) in absence of the state constraint $I(t) \leq I_{max}$ with solutions of the problem subjected to the state constraint. Our principal focus is on examining the state trajectories of Asymptomatics $A(t)$, Infected $I(t)$ and Deaths $D(t)$, since they reflect the severity of the epidemics. We display only the adjoint variable $\lambda_I(t)$ which has jumps at the junction points with a boundary arc $I(t) = I_{max}$. All other adjoint variables are continuous and vanish at the final time; see (34), (35). We start with solving the optimal control problem without the state constraint $I(t) \leq I_{max}$. The resulting boundary value problem (41) can be solved either by the Forward-Backward-Sweep-Mathod (FBSM) [40] or by the BVP4c solver in Matlab. Since the FBSM method converges only for a sufficiently small time interval, we prefer to use the solver BVP4c, which is a fourth-order integration method is implemented for the ODE system. The optimal control problem with state constraint is solved by discretization methods. The discretized control problem gives rise to a large-scale nonlinear optimization problem which is conveniently formulated using the Mathematical Programming Language AMPL developed by Fourer et al. [19]. AMPL can be linked to several optimization codes. In our computations, we have used the primal-dual interior point code IPOPT developed by Wächter [67]. The AMPL program can be directly submitted to the NEOS server; see [47]. As integration method we use either the Euler implicit method or the trapezoidal rule. We choose the number $N = 700$, resp.

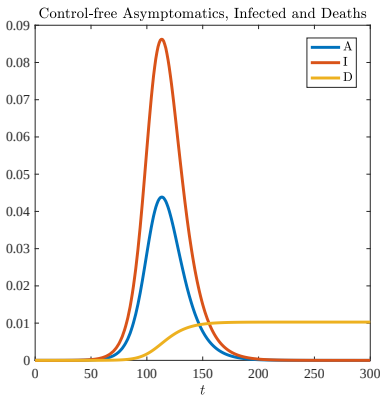

FIGURE 2. Uncontrolled Covid-19 spread according to SEAIRD system (2)-(7). Infected population $I(t)$ reaches a peak of almost 0.09 after 114 days.

$N = 2000$, for the time horizon $T = 70$, resp. $T = 200$, and prescribe the tolerance $tol = 10^{-8}$ in all computations. An alternative numerical method is provided by the DIDO solver which is based on a pseudospectral approach [56]. Before inspecting the controlled virus spread, we show the solution of the SEAIRD dynamics (2)-(7) in absence of any control policy, i.e $u(t) \equiv 1$; see Figure 2. Our analysis begins with considering three different scenarios corresponding to different initial conditions when restrictions policies begin to be imposed. For convenience we recall the new initial conditions (17)-(19) that correspond to a mild, a more severe and a very severe spread out of the virus.

Case 1. Integration of (2)–(7), (9) with $u(t) \equiv 1$ up to time $T_0 = 55$ days.

$$X_0 = [0.9979, 7.713\cdot 10^{-4}, 1.941\cdot 10^{-4}, 3.841\cdot 10^{-4}, 6.463\cdot 10^{-4}, 8.58904\cdot 10^{-6}]. \quad (42)$$

Case 2. Integration of (2)–(7), (9) with $u(t) \equiv 1$ up to time $T_0 = 65$ days.

$$X_0 = [0.9932, 0.002614, 6.601 \cdot 10^{-4}, 0.001306, 0.002208, 2.934 \cdot 10^{-5}]. \quad (43)$$

Case 3. Integration of (2)–(7), (9) with $u(t) \equiv 1$ up to time $T_0 = 70$ days.

$$X_0 = [0.9873, 0.004853, 0.001229, 0.002434, 0.004138, 5.499 \cdot 10^{-5}] \quad (44)$$

First, we investigate the optimal control problem in the absence of the state constraint for the time interval of $T = 70$ days. Then, we investigate the state-constrained problem both for the short terminal time $T = 70$ days and for the much larger terminal time $T = 200$.

5.1. **Case 1: X_0 after 55 days from the first exposure.** After 55 days from the first exposure, the number of exposed people is less than 800 in one million people. Thus, we can intuitively think that it is not a severe situation which needs immediately strict confinement. We will see that the results are consistent with this claim.

5.1.1. *Unconstrained problem for* $T = 70$. We consider the unconstrained solution omitting the condition $I(t) \leq I_{max} = 0.005$. Hence, we can solve the boundary value problem (41). Figure 3 displays the solution. Figure 3(A) shows that the optimal

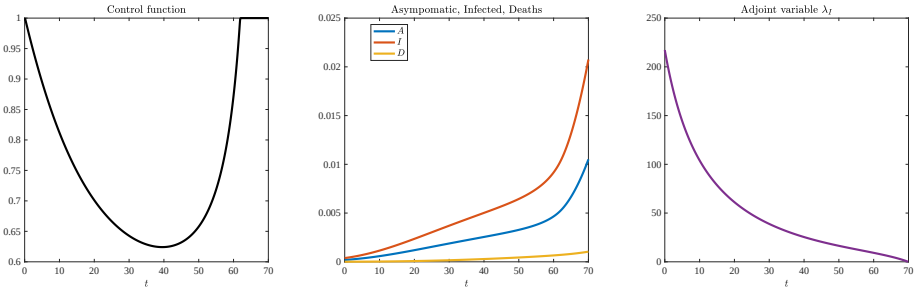

(A) (B) (C)

FIGURE 3. **Case 1**: Optimal solution for $T = 70$ without state constraint $I(t) \leq 0.005$. (A) control $u(t)$, (B) asymptomatic $A(t)$, infected $I(t)$ and deaths $D(t)$. (C) adjoint variable $\lambda_I(t)$.

policy begins with total freedom, decreases until it reaches the most restricted level $u = 0.62$ after 41 days, and then gradually increases to reach the maximum level $u = 1$ at day 62. It is not surprising that the policy is not restrictive at beginning, since the initial conditions do not yet provide a serious scenario. We find

$$\max\{I(t) \,|\, 0 \leq t \leq T\} = I(T) = 0.0208.$$

Hence, the state constraint $I(t) \leq I_{max}$ will become active for any bound $I_{max} < 0.02$. Then we will either have $I(T) = I_{max}$ or a touching point $t_s \in (0, T)$ with $I(t_s) = I_{max}$ or a boundary arc $I(t) = I_{max}$ for $t_1 \leq t \leq t_2$ with $0 < t_1 < t_2 < T$. This occurs also in Case 2 and Case 3 in absence of the state constraint, as we will see below. The control decreases in the first period rather than thereafter which is due to the presence of the discount factor in the objective functional. Infected people exceed the value 0.01 in 63 days and then double in a few days. In this setting, we obtain $D(T) = 0.001$ compared to $D(T) = 0.01$ that would be without any restrictions. Under control, asymptomatics $A(t)$ assumes its maximum value at the final time, $A(T) = 0.01$, while in the analogous setting without control, the maximum value of asymptomatics is 0.044; see Figure 2. Notice that the final level of infected people under restrictions is the same at day 30 in the scenario without any control and then increases more than four times along the interval. The optimal cost is $F = 3.6674$. The final value $\lambda_I(T) = \eta_T = 0$ is consistent with the transversality condition (34). We also observe that the adjoint variable $\lambda_I(t)$ depicted in Figure 3 is consistent with the condition (35), because the absence of the state constraint does not produce any jumps. Also, in all unconstrained cases reported below we will see that $\lambda_I(t)$ is a continuous function with $\lambda_I(T) = 0$.

5.1.2. *Constrained solution for* $T = 70$. We now turn to the case of the problem with the same initial condition but with the additional state constraint $I(t) \leq I_{max} = 0.005$. As shown in Figure 4, the control policy starts almost from $u = 1$ and decreases until day 58 at the control level $u = 0.505$ and then reaches the

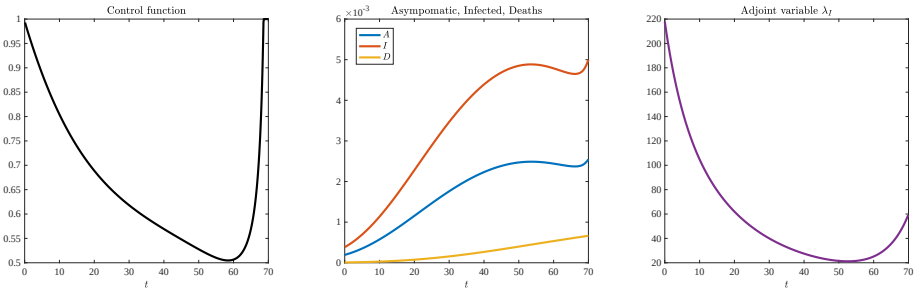

(A) (B) (C)

FIGURE 4. **Case 1**: Solution for terminal time $T = 70$ with state constraint $I(t) \leq 0.005$. (A) control $u(t)$. (B) asymptomatics $A(t)$, infected $I(t)$ and deaths $D(t)$. (C) adjoint variable $\lambda_I(t)$.

total freedom in the last days of the time period. Notice that the terminal values $I(T) = 0.005$ of infected, $A(T) = 0.0025$ of asymptomatic and $D(T) = 6.6 \cdot 10^{-4}$ of deaths are significantly smaller than the terminal values $I(T) = 0.0208, A(T) = 0.01, D(T) = 0.001$ without state constraint; see Figure 4(B) and Figure 2. It is not surprising that the total social cost $F = 3.89148$ is higher than $F = 3.6674$ without the threshold I_{max}. We also notice that the state constraint is only active at $t = T$, since $I(T) = 0.005$ and $I(t) < 0.005$ for $t < T$. The transversality condition (34) holds with $\lambda_I(T) = \nu_T = 60$, but the adjoint variable λ_I does not have any jumps.

5.1.3. *Constrained solution for $T = 200$.* The control function and the asymptomatic, infected and deaths for the terminal time $T = 200$ are depicted in Figure 5. Note that, as in Figure 4(A) the optimal policy starts with total freedom and

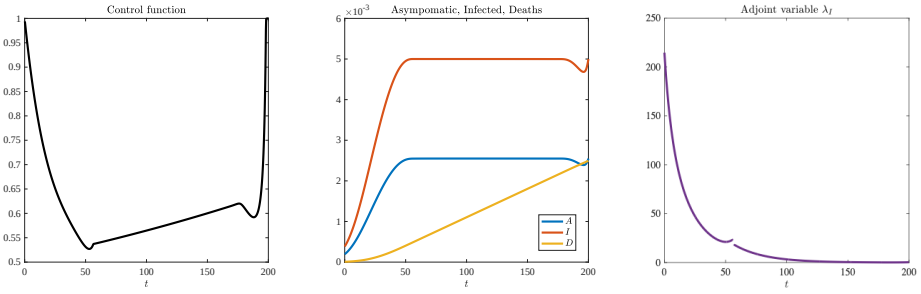

(A) (B) (C)

FIGURE 5. **Case 1**: Solution for $T = 200$ with state constraint $I(t) \leq 0.005$. (A) control $u(t)$ with boundary interval $[56.2, 178]$. (B) asymptomatics $A(t)$, infected $I(t)$ and deaths $D(t)$. (C) adjoint variable $\lambda_I(t)$.

it reaches its minimum value at the level $u = 0.53$. Then it settles between the values $u = 0.55$ and $u = 0.6$ for about 4 months. In Figure 5(B) we notice that the

constraint is active in the boundary interval $[t_1, t_2]$, where $t_1 = 56.2$ and $t_2 = 178$, and at the final time T. Even on this large time interval the control is still able to hold down the number of infected people. Moreover, at the final time we have $A(T) = 2.55 \cdot 10^{-3}$ and $D(T) = 2.5 \cdot 10^{-3}$. The transversality condition (34) is satisfied with $\lambda_I(T) = \nu_T = 0.3$. Note also that, according to (35), the adjoint function $\lambda_I(t)$ presents a jump at $t = t_1$. The rapid decrease of $\lambda_I(t)$ to zero does not make evident the additional jump at $t = t_2$. In summary, we conclude that after a transition period staring on freedom the policy is restrictive for a long time and it leads to total freedom again at the end of the time interval. The final cost of this scenario is $F = 4.40835$, which is significantly higher then $F = 3.89148$ in the analogous shorter time setting for $T = 70$.

5.2. **Case 2: X_0 after 65 days from the first exposure.** Computing the SEAIRD system (2)-(7) with control $u(t) = 1$, we observed that after 65 days from the first exposure, the number of exposed people is 2600 in one million people. Thus, they have tripled in 10 days from the setting in Case 1. We expect the optimal control to be more restrictive and the optimal cost to increase.

5.2.1. *Unconstrained solution for $T = 70$.* Omitting the state constraint $I(t) \leq I_{max} = 0.005$ we obtain the solution displayed in Figure 6. Figure 6(A) shows that

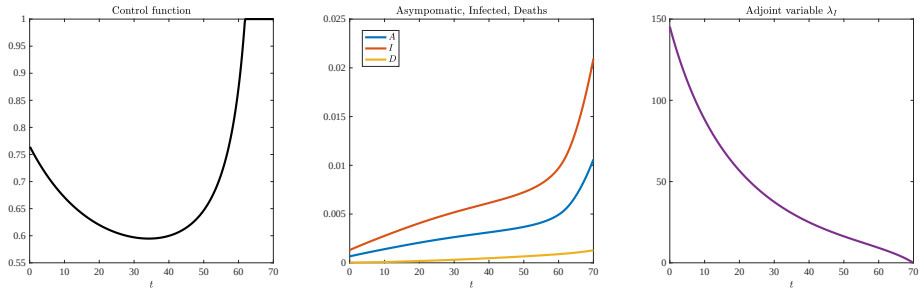

(A) (B) (C)

FIGURE 6. **Case 2**: Solution for $T = 70$ without state constraint $I(t) \leq I_{max} = 0.005$. (A) control $u(t)$. (B) asymptomatics $A(t)$, infected $I(t)$ and deaths $D(t)$. (C) adjoint variable $\lambda_I(t)$.

the optimal control of the problem without state constraint starts from the level $u = 0.76$. It decreases until the most restricted level $u = 0.59$ is reached after 34 days and then increases to reach the total freedom $u = 1$ after 63 days. We also see that the trajectories are similar to those depicted in Figure 3 even though the control is quite different, in particular at the initial time. After day 62 the number of infected people doubles in a few days. The final values of $I(T)$, $A(T)$ and $D(T)$ are almost the same as in the scenario of Case 1. Because of the absence of the state constraint, we have $\lambda_I(T) = \nu_T = 0$. The optimal cost is $F = 5.64477$.

5.2.2. *Constrained solution for $T = 70$.* In Figure 7(A) we observe that the control starts with the value $u = 0.76$ and it reaches the minimum value 0.51 after 58 days. The state constraint is active for $t_1 \leq t \leq t_2$ and at $t = T$, where $t_1 = 43.2$

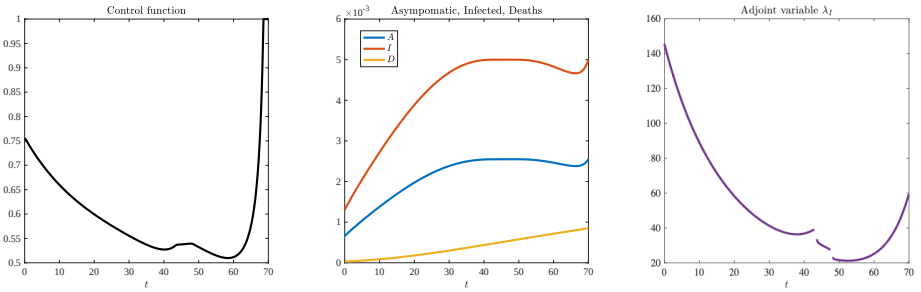

(A) (B) (C)

FIGURE 7. **Case 2:** Solution for $T = 70$ with state constraint $I(t) \leq I_{max} = 0.005$. (A) control $u(t)$ with boundary interval $[43.2, 48]$. (B) asymptomatics $A(t)$, infected $I(t)$ and deaths $D(t)$. (C) adjoint variable $\lambda_I(t)$.

and $t_2 = 48$. The adjoint variable $\lambda_I(t)$ exhibits jumps at t_1 and t_2 in agreement with (35). In view of the transversality condition (34), we find the terminal value $\lambda_I(T) = \nu_T = 59.2$. Compared to the situation without state constraint in Figure 6(B) we obtain the terminal values $D(T) = 8.5 \cdot 10^{-4}$, $A(T) = 2.55 \cdot 10^{-3}$. The total cost is $F = 5.8888$ rather than $F = 5.64477$ without the state constraint.

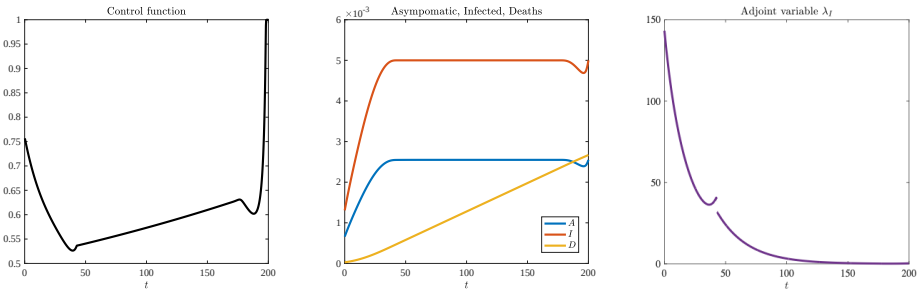

(A) (B) (C)

FIGURE 8. **Case 2:** Solution for $T = 200$ with state constraint $I(t) \leq 0.005$. (A) control $u(t)$ with boundary interval $[42.5, 178]$. (B) asymptomatics $A(t)$, infected $I(t)$ and deaths $D(t)$. (C) adjoint variable $\lambda_I(t)$.

5.2.3. *Constrained solution for* $T = 200$. As in the shorter time interval, in Figure 8(A) we notice that the initial condition strongly affects the optimal control, specifically at smaller times. Indeed, compared to Case 1 in Figure 5(A), where the policy starts with total freedom, the initial control is $u(0) \approx 0.75$. Then it reaches the minimum level $u = 0.53$ after 40 days, and then stays in a neighborhood of 0.55 for a long time before sharply increasing at the end. As expected, the state constraint

$I(t) \leq 0.005$ saturates on $[t_1, t_2]$ and at $t = T$ where $t_1 = 42.5$ and $t_2 = 175$; see Figure 8(B). According to (35), the adjoint function λ_I has jumps at t_1 and t_2. The rapid decrease of $\lambda_I(t)$ to zero does not make evident the additional jump at $t = t_2$. In view of condition (34), $\lambda_I(T) = \nu_T = 0.3$. In comparison with the same scenario in a shorter time horizon, see Figure 7(B), the final value $A(T) = 2.55 \cdot 10^{-3}$ is the same, while the final number of deaths is significantly higher, $D(T) = 2.7 \cdot 10^{-3}$. This result demonstrates the impact of implementing a policy only 10 days later. Indeed, compared to the scenario where X_0 is 10 days before, the number of deaths increases three times despite the action of a more restrictive policy that is still able to hold down the trajectory $I(t)$. In this case the final cost is $F = 6.3967$, whereas we get $F = 5.8888$ for the shorter time horizon $T = 70$ and $F = 4.40835$ for the initial condition corresponding to 10 days earlier.

5.3. **Case 3: X_0 after 70 days from the first exposure.** After 70 days from the first exposure, the number of exposed individuals are about 4800 in one million people. It means that, after only 5 days after the previous setting, the spread of virus has almost doubled and it becomes quite severe. Again, we begin by considering the optimal control problem in the absence of the state constraint.

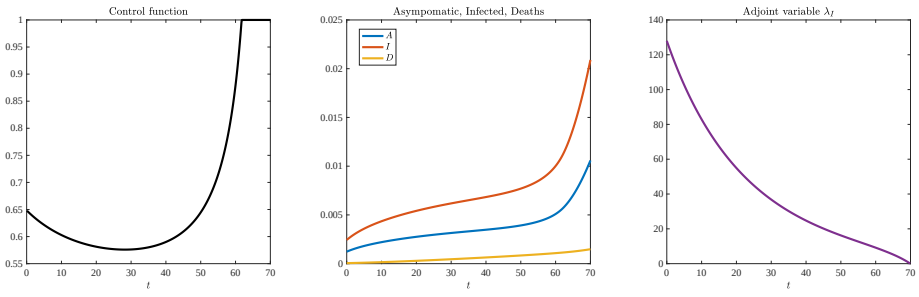

(A) (B) (C)

FIGURE 9. **Case 3:** solution for $T = 70$ without state constraint $I(t) \leq I_{max} = 0.005$. (A) control $u(t)$. (B) asymptomatics $A(t)$, infected $A(t)$ and deaths $D(t)$. (C) adjoint variable $\lambda_I(t)$.

5.3.1. *Unconstrained solution for $T = 70$.* Figure 9(A) demonstrates that the later government acts the more restrictive the policy must be on the initial period. Indeed, we observe that the control starts with the level $u = 0.65$ until it achieves the minimum level $u = 0.58$ in about one month. Then $u(t)$ gradually increases to total freedom after 63 days. Once again, the trajectories of asymptomatics, infected and deaths depicted in Figure 9(B) show that the control is able to satisfy the state constraint $I(t) \leq 0.005$ on the whole time interval. The final cost is $F = 7.02614$. It is not surprising that the optimal cost is significantly increasing as the policy start is delayed. We refer to Figure 3 and Figure 6 for the discussion about terminal state values, since they are similar to those in previous settings.

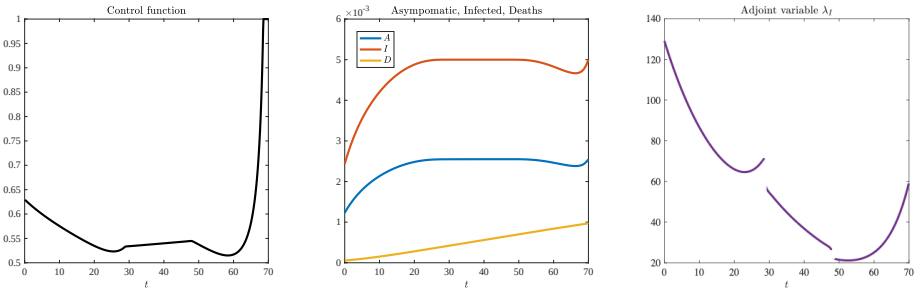

(A) (B) (C)

FIGURE 10. **Case 3:** Solution for $T = 70$ with state constraint $I(t) \leq I_{max} = 0.005$. (A) control $u(t)$ with boundary interval $[28.5, 48]$. (B) asymptomatics $A(t)$, infected $I(t)$ and deaths $D(t)$. (C) adjoint variable $\lambda_I(t)$.

5.3.2. *Constrained solution for* $T = 70$. The initial control is $u = 0.63$; the control stays in a neighborhood of $u = 0.55$ for a long period. It reaches its minimum value $u = 0.51$ and then sharply increases up to total freedom in 10 days; see Figure 10(A). Notice that asymptomatic, infected and deaths trajectories are dramatically reduced when compared to Figure 9(B). The infected compartment assumes its maximum value for $t \in [t_1, t_2]$ and in $t = T$, where $t_1 = 28.5$ and $t_2 = 48$. Consistently with (35), the adjoint function $\lambda_I(t)$ exhibits two jump points at t_1 and t_2. The final value of transversality condition (34) is $\lambda_I(T) = \nu_T = 59$. Since the initial condition in Case 3 describes a severe epidemic outbreak, the final state of deaths increases $D(T) = 0.001$. The final cost for implementing the optimal restriction policy is now $F = 7.29966$ compared to $F = 7.02614$ without state constraint.

5.3.3. *Constrained solution for* $T = 200$. We turn to the last case where we assume that initial condition corresponds to a severe epidemic spread and the time interval is much longer. This situation is the most critical one to bring under control, thus we expect that the optimal cost is the highest compared to all scenarios considered before. In Figure 11(A) we notice that the initial control value is lower than in the previous setting. Indeed, it starts from 0.63 and decreases to its minimum value $u = 0.52$ in about 25 days. Thus, it will remain between 0.55 and 0.65 for 5 months and it sharply increases to total freedom only in the last days. The number of infected saturates in about 20 days. Indeed, Figure 11(B) shows that the constraint is active in $[t_1, t_2]$ and $t = T$, with $t_1 = 28.4$ and $t_2 = 178$. According to condition (35), the adjoint variable $\lambda_I(t)$ has two jump points in t_1 and t_2. The rapid decrease of $\lambda_I(t)$ to zero does not make evident the additional jump at $t = t_2$. The final value of additional multiplier is $\lambda_I(T) = \nu_T = 0.3$, see condition (34). The final size of state variables are $A(T) = 2.55 \cdot 10^{-3}$ and $D(T) = 2.8 \cdot 10^{-3}$. In particular, we remark that the number of dead people is higher than twice the number of deaths in case $T = 70$; see Figure 10(B). The optimal social cost is $F = 7.80120$ compared to $F = 7.29966$ in 70 days and compared to $F = 6.3967$ for the initial condition chosen 5 days earlier in Case 2.

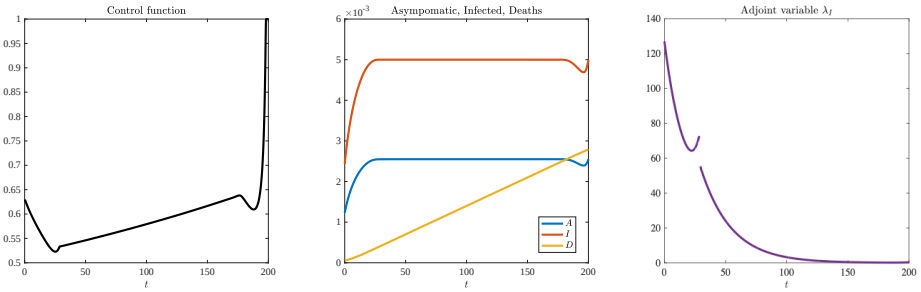

(A) (B) (C)

FIGURE 11. **Case 3**: Solution for $T = 200$ with state constraint $I(t) \leq 0.005$. (A) control $u(t)$ with boundary interval $[28.4, 178]$. (B) asymptomatics $A(t)$, infected $I(t)$ and deaths $D(t)$. (C) adjoint variable $\lambda_I(t)$.

5.3.4. *Approximative constrained solution for* $T = 200$. We pointed out that in practice it is difficult to implement the *continuous* controls, that provide idealized policies, obtained in the previous sections. An *approximative* control which is piecewise constant on a prescribed segmentation of the interval $[0, T]$ can be designed in the following way. Consider the following times of changing the lockdown strategy,

$$t_0 = 0,\ t_1 = 50,\ t_2 = 100,\ t_3 = 125,\ t_4 = 150,\ t_5 = 175,\ t_6 = 200,$$

and assume that the *approximative* control $u_a(t)$ is piecewise constant with

$$u_a(t) = c_i \quad \text{for} \quad t_{i-1}^+ \leq t \leq t_i^- \quad (i = 1, \ldots, 6). \tag{45}$$

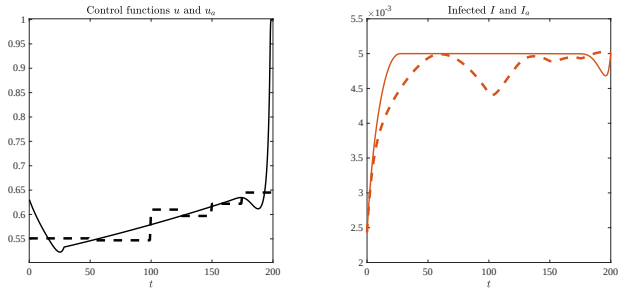

(A) (B)

FIGURE 12. **Case 3**: Optimal and approximative solution for $T = 200$ on 6 segments of $[0, T]$. (A) optimal control $u(t)$ and approximative control $u_a(t)$. (B) infected $I(t)$ and approximative infected $I_a(t)$.

The constant values $c_i \in [0.01, 1]$, $i = 1, \ldots, 6$, in (45) are optimized under the state constraint $I(t) \leq 0.005$. The optimization approach AMPL/IPOPT yields the

constant control values

$$c_1 = 0.551, \quad c_2 = 0.547, \quad c_3 = 0.609, \quad c_4 = 0.597, \quad c_5 = 0.622, \quad c_6 = 0.644,$$

and the approximative cost $F_a = 7.856$ that differs only slightly from the optimal cost $F = 7.801$. The optimal and approximative controls $u(t)$ and $u_a(t)$, resp., optimal and approximative infected $I(t)$ and $I_a(t)$ are shown in Figure 12. Note that the lockdown rate $c_6 = 0.644$ in the terminal interval $[175, 200]$ is still quite restrictive. This value can be improved by introducing an additional control value c_7 on the small terminal segment $[195, 200]$. Here, we obtain the value $c_7 = 0.917$ which is close to the control value $u = 1$ representing total freedom.

We summarize the main results in the table below, recalling that the initial condition is referred to the starting day of control with respect to the first case of virus exposure.

TABLE 2. Numerical results for the 3 scenarios of initial conditions (42), (43), (44).

X_0	T	$I \le I_{max}$	min $u(t)$	F	$I(T)$	$A(T)$	$D(T)$	ν_T
55	70	✗	0.62	3.6674	0.0208	0.01	0.001	0
55	70	✓	0.51	3.8915	0.005	$2.55 \cdot 10^{-3}$	$6.6 \cdot 10^{-4}$	60
55	200	✓	0.53	4.4084	0.005	$2.55 \cdot 10^{-3}$	$2.5 \cdot 10^{-3}$	0.3
65	70	✗	0.59	5.6448	0.0209	0.01	0.001	0
65	70	✓	0.51	5.8888	0.005	$2.55 \cdot 10^{-3}$	$8.5 \cdot 10^{-4}$	59.2
65	200	✓	0.53	6.3967	0.005	$2.55 \cdot 10^{-3}$	$2.7 \cdot 10^{-3}$	0.3
70	70	✗	0.58	7.0261	0.0209	0.0106	0.0015	0
70	70	✓	0.51	7.2997	0.005	$2.55 \cdot 10^{-3}$	0.001	59
70	200	✓	0.52	7.8012	0.005	$2.55 \cdot 10^{-3}$	$2.8 \cdot 10^{-3}$	0.3

6. **Conclusion.** We considered an optimal control model for a SEAIRD epidemiological system, where a cost functional to be minimized represents a trade-off between economic and human losses; see Aspri et al [5]. Since a percentage of infected people needs hospitalization and the Intensive Care Units (ICU) are limited, overcrowding of ICUs can be avoided by imposing a state constraint on the number of infected people. The state constraint is of second order which poses a number of theoretical and numerical challenges. Hence, the proposed state-constrained optimal control problem takes into account the three main aspects in a real epidemic framework: economy, deaths and hospital capacity. We considered three scenarios for initial conditions representing a mild, an advanced and a severe spread of an epidemic. Firstly, we proved the existence of an optimal solution for all three scenarios. Then we evaluated the necessary optimality conditions of the Pontryagin Maximum Principle which lead to a system of algebraic and ordinary differential equations. The multiplier associated with the state constraint is a function of bounded variation. It could be shown that this function has a density on boundary arcs and leads to jumps of the adjoint variable at junction times. We used different numerical methods to solve the optimal control problem. Omitting the state constraint, we solved the boundary-value problem arising from the Minimum Principle. Solutions

of the state-constrained control problem are obtained by discretizing the control problem and applying large-scale optimization methods. For the three scenarios of initial conditions we studied the solutions for smaller and larger time horizons. The numerical results for altogether nine different scenarios are compared in Table 2. Comparing the optimal cost values we see that it is beneficial to compute the control on the large time interval with $T = 200$ instead of $T = 70$, since the cost is increased only by approximatively by 10%. Another point is how the control and cost change in relation to initial conditions. As expected, the more severe the initial situation is the more expensive is the control action. This suggests that a prompt action would reduce the cost in addition to the virus spread. Furthermore, comparing all scenarios the maximum limitation of freedom obtained is around 50%. It provides a moderate restriction, considering that it is reached for rather short intermediate time periods. This approach provides the tools to handle other additional issues. For example, we did not impose conditions on the final state. Our aim was to flatten the curve of infected people without prescribing a terminal state or the almost total eradication of the virus. We can ask which is the cost for the eradication compared to maintaining the spread under a threshold. From a research perspective, it would be interesting to analyze the same optimal control setting approximating the continuous control by a piecewise constant control with only a few arcs and then compare the objective values, as displayed in the example (12a)-(12b). Another task could be to take into account the same formulation with an additional control of vaccination and its related cost in order to combine pharmaceutical and non-pharmaceutical policies.

Funding. This work was supported by the Italian Ministry for University and Research (MUR) through the PRIN 2020 project "Integrated Mathematical Approaches to Socio-Epidemiological Dynamics" (No. 2020JLWP23, CUP: E15F21005420006).

Acknowledgments. We would like to thank both referees for comments which helped us improve the presentation of the optimal control problem.

REFERENCES

[1] D. Acemoglu, V. Chernozhukov, I. Werning, M. Whinston, Optimal targeted lockdowns in a multi-group SIR model, *American Economic Review: Insights*, **3** (2021), 487-502.

[2] Z. Abbasi, I. Zamani, A. H. A. Mehra, M. Shafieirad, A. Ibeas, Optimal control design of impulsive SQEIAR epidemic models with application to COVID-19, *Chaos, Solitons and Fractals*, **139** (2020),110054.

[3] L. J. S. Allen, An Introduction to Stochastic Epidemic Models, *Mathematical Epidemiology. Lecture Notes in Mathematics* Springer Berlin Heidelberg, 2008, 81–130.

[4] J. K. K. Asamoah, Z. Jin, G. Q. Sun, B. Seidu, E. Yankson, A. Abidemi, F. T. Oduro, S. E. Moore, E. Okyere, Sensitivity assessment and optimal economic evaluation of a new COVID-19 compartmental epidemic model with control interventions, *Chaos, Solitons and Fractals*, **146** (2021), 110885.

[5] A. Aspri, E. Beretta, A. Gandolfi, E. Wasmer, Mortality containment vs. economics opening: Optimal policies in a SEIARD model, *Journal of Mathematical Economics*, **93** (2021).

[6] J. Bauer, D. Brüggmann, D. Klingelhöfer, et al, Access to intensive care in 14 European countries: a spatial analysis of intensive care need and capacity in the light of COVID-19, *Intensive Care Med*, **46** (2020), 2026-2034.

[7] H. Behncke, Optimal control of deterministic epidemics, *Optimal Control Applications and Methods*, **21** (2000), 269-285.

[8] M. H. A. Biswas, L. T. Paiva, M. R. De Pinho, A SEIR model for control of infectious diseases with constraints, *Mathematical Biosciences and Engineering*, **11** (2014), 761-784.

[9] G. Bonaccorsi, F. Pierri, M. Cinelli, A. Flori, A. Galeazzi, F. Porcelli, A. L. Schmidt, C. M. Valensise, A. Scala, W. Quattrociocchi, F. Pammolli, Economic and social consequences of human mobility restrictions under COVID-19, *Proceedings of the National Academy of Sciences of the United States of America*, **117** (2020), 15530-15535.

[10] J. P. Caulkins, D. Grass, G. Feichtinger, R. F. Hartl, P. M. Kort, A. Prskawetz, A. SeidL, S. Wrzaczekd, The optimal lockdown intensity for COVID-19, *Journal of Mathematical Economics*, **93** (2021), 102489.

[11] L. Cesari, *Optimization Theory and Applications. Problems with Ordinary Differential Equations*, Springer-Verlag, 1983.

[12] A. Charpentier, R. Elie, M. Laurière, V. C. Tran, COVID-19 pandemic control: balancing detection policy and lockdown intervention under ICU sustainability. *Mathematical Modelling of Natural Phenomena*, **15** (2020).

[13] W. Choi, E. Shim, Optimal strategies for social distancing and testing to control COVID-19, *Journal of Theoretical Biology*, **512** (2021), 110568.

[14] L. Cianfanelli, F. Parise, D. Acemoglu, G. Como, A. Ozdaglar, Lockdown interventions in SIR model: Is the reproduction number the right control variable?, *60th IEEE Conference on Decision and Control (CDC)* 2021, 4254-4259.

[15] M. R. De Pinho, I. Kornienko, H. Maurer, Optimal control of a SEIR model with mixed constraints and L1 cost, *Lecture Notes in Electrical Engineering*, 321 LNEE, 2015, 135-145.

[16] N. Donthu, A. Gustafsson, Effects of COVID-19 on business and research, *Journal of Business Research*, **117** (2020), 284-289.

[17] F. Fernández-Aranda, M. Casas, L. Claes, D. C. Bryan, A. Favaro, R. Granero, C. Gudiol, S. Jiménez-Murcia, A. Karwautz, D. Le Grange, J. M. Menchón, K. Tchanturia, J. Treasure, COVID-19 and implications for eating disorders, *European Eating Disorders Review*, **28** (2020), 239-245.

[18] S. Flaxman, S. Mishra, A. Gandy, H. J. T. Unwin, T. A. Mellan, H. Coupland, C. Whittaker, Estimating the effects of non-pharmaceutical interventions on COVID-19 in Europe, *Nature*, **584** (2020), 257-261.

[19] R. Fourer, M. Gay, B. Kernighan, AMPL: A Modeling Language for Mathematical Programming, *Management Science*, **36** (1990), 519-554.

[20] K. Fister, S. Lenhart, J. McNally, Optimizing chemotherapy in an HIV model, *Electron. J. Differ. Equat*, **1998** (1998), 1-12.

[21] A. Gandolfi, A. Aspri, E. Beretta, K. Jamshad, M. Jiang, A new threshold reveals the uncertainty about the effect of school opening on diffusion of Covid-19, *Scientific Reports* **12** (2022).

[22] M. Gatto, E. Bertuzzo, L. Mari, S. Miccoli, L. Carraro, R. Casagrandi, A. Rinaldo, Spread and dynamics of the COVID-19 epidemic in Italy: Effects of emergency containment measures, *Proceedings of the National Academy of Sciences*, **117** (2020), 10484-10491.

[23] G. Giordano, F. Blanchini, R. Bruno, P. Colaneri, A. Di Filippo, A. Di Matteo, M. Colaneri, Modelling the COVID-19 epidemic and implementation of population-wide interventions in Italy, *Nature Medicine*, **26** (2020), 855-860.

[24] J. A. Gondim, L. Machado, Optimal quarantine strategies for the COVID-19 pandemic in a population with a discrete age structure, *Chaos, Solitons and Fractals*, **140** (2020), 110166.

[25] R. Hartl, S. Sethi, R. Vickson, A survey of the Maximum Principles for Optimal Control Problems with State Constraints *SIAM Review*, **37** (1995), 181-218.

[26] H. W. Hethcote, Mathematics of infectious diseases, *SIAM Review*, **42** (2000), 599-653

[27] M. Kantner, T. Koprucki, Beyond just "flattening the curve": Optimal control of epidemics with purely non-pharmaceutical interventions, *Journal of Mathematics in Industry*, **10** (2020).

[28] D. H. Jacobson, M. M. Lele, and J. L. Speyer, New necessary conditions of optimality for control problems with state-variable inequality constraints, *J. Math. Anal. Appl.*, **35** (1971), 255-284.

[29] A. J. Kucharski, T. W. Russell, C. Diamond, Y. Liu, J. Edmunds, S. Funk et al., Early dynamics of transmission and control of COVID-19: a mathematical modelling study, *The Lancet Infectious Diseases*, **20** (2020), 553-558.

[30] S. Lenhart, J. Workman, *Optimal Control Applied to Biological Models*, Mathematical and Computational Biology Series, Chapman and Hall/CRC, 2007.

[31] G. B. Libotte, F. S. Lobato, G. M. Platt, A. J. Silva Neto, Determination of an optimal control strategy for vaccine administration in COVID-19 pandemic treatment, *Computer Methods and Programs in Biomedicine*, **196** (2020).

[32] F. Lin, K. Muthuraman, M. Lawley, An optimal control theory approach to non-pharmaceutical interventions, *BMC Infectious Diseases*, **10** (2010).
[33] Z. Liu, P. Magal, O. Seydi, G. Webb, A COVID-19 epidemic model with latency period, *Infectious Disease Modelling*, **5** (2020), 323-337.
[34] X. Lü, H. Hui, F. Liu, Y. Bai, Stability and optimal control strategies for a novel epidemic model of COVID-19, *Nonlinear Dynamics*, **106** (2021), 1491-1507.
[35] A. Mahajan, N. A. Sivadas, R. Solanki, An epidemic model SIPHERD and its application for prediction of the spread of COVID-19 infection in India, *Chaos, Solitons and Fractals*, **140** (2020), 110156.
[36] M. Mandal, S. Jana, S. K. Nandi, A. Khatua, S. Adak, T. Kar, A model based study on the dynamics of COVID-19: Prediction and control, *Chaos, Solitons and Fractals*, **136** (2020),109889.
[37] H. Maurer, *On the minimum principle for optimal control problems with state constraints*, Schriftenreihe des Rechenzentrums der Universität Münster Nr. 41, Münster, 1979.
[38] C. Maringe, J. Spicer, M. Morris, A. Purushotham, E. Nolte, R. Sullivan, B. Rachet, A. Aggarwal, The impact of the COVID-19 pandemic on cancer deaths due to delays in diagnosis in England, UK: a national, population-based, modelling study, *The Lancet Oncology*, **21** (2020), 1023-1034.
[39] L. Matrajt, J. Eaton, T. Leung, E. R. Brown, Vaccine optimization for COVID-19: Who to vaccinate first?, *Science Advances*, **7** (2021), 1374.
[40] M. McAsey, L. Mou, W. Han, Convergence of the Forward-Backward Sweep Method in Optimal Control, *Comput Optim Appl*, **53** (2012), 207-226.
[41] L. Miclo, D. Spiro, J. Weinbull, Optimal epidemic suppression under an ICU constraint: an analytical solution, *Journal of Mathematical Economics*, **101** (2022), 102669.
[42] D. Moreira, M. P. Da Costa, The impact of the Covid-19 pandemic in the precipitation of intimate partner violence, *Int J Law Psychiatry*, **71** (2020), 101606.
[43] R. Morton, K. Wickwire, On the Optimal Control of a Deterministic Epidemic, *Advances in Applied Probability*, **6** (1974), 622-635.
[44] M. Natilli, A. Rossi, A. Trecroci, L. Cavaggioni, G. Merati, D. Formenti, The long-tail effect of the COVID-19 lockdown on Italians' quality of life, sleep and physical activity, *Scientific Data*, **9**, 250 (2022).
[45] F. Ndaïrou, I. Area, J. J. Nieto, D. F. Torres, Mathematical modeling of COVID-19 transmission dynamics with a case study of Wuhan, *Chaos, Solitons and Fractals*, **135** (2020).
[46] R. M. Neilan, S. M. Lenhart, An Introduction to Optimal Control with an Application in Disease Modeling, *DIMACS Series in Discrete Mathematics*, **75** (2010), 67-81.
[47] https://neos-server.org/neos/index.html
[48] M. Nicola, Z. Alsafi, C. Sohrabi, A. Kerwan, A. Al-Jabir, C. Iosifidis, M. Agha, R. Agha, The socio-economic implications of the coronavirus pandemic (COVID-19): A review, *Int J Surg*, **78** (2020), 185-193.
[49] R. Pastor-Satorras, C. Castellano, P. Van Mieghem, A. Vespignani, Epidemic processes in complex networks, *Reviews of Modern Physics*, **87** (2015).
[50] N. Perra, D. Balcan, B. Gonçalves, A. Vespignani, Towards a Characterization of Behavior-Disease Models, *PLOS ONE*, **6** (2011), 1-15.
[51] T. A. Perkins, G. España, Optimal Control of the COVID-19 Pandemic with Non-pharmaceutical Interventions, *Bulletin of Mathematical Biology*, **82** (2020), 118.
[52] L. Pontryagin, G. Boltyanskii, R. Gamkrelidze, E. Mishchenko, *Mathematical Theory of Optimal Processes*, NewYork, 1964.
[53] K. Prem, Y. Liu, T. W. Russell, A. J. Kucharski, R. M. Eggo, N. Davies, et al, The effect of control strategies to reduce social mixing on outcomes of the COVID-19 epidemic in Wuhan, China: a modelling study, *The Lancet Public Health*, **5** (2020), e261-e270.
[54] A. Remuzzi, G. Remuzzi, COVID-19 and Italy: what next?, *The Lancet*, **395** (2020), 1225-1228.
[55] Q. Richard, S. Alizon, M. Choisy, M. T. Sofonea, R. Djidjou-Demasse, Age-structured non-pharmaceutical interventions for optimal control of COVID-19 epidemic, *PLoS Computational Biology*, **17** (2021), e1008776.
[56] I. M. Ross, *A Primer on Pontryagin's Principle in Optimal Control* 2^{nd} edition, Collegiate Publishers, San Francisco, 2015.
[57] S. Saha, G. Samanta, Modelling the role of optimal social distancing on disease prevalence of COVID-19 epidemic, *International Journal of Dynamics and Control*, **9** (2021), 1053-1077.

[58] S. Sethi, P. Staats, Optimal control of some simple deterministic epidemic models, *The Journal of the Operational Research Society*, **29** (1978), 129-136.
[59] H. Schättler, U. Ledzewicz, Optimal Control for Problems with a Quadratic Cost Functional on the Therapeutic Agents in *Optimal Control for Mathematical Models of Cancer Therapies*, New York, Springer New York, 2015, 141-170.
[60] O. Sharomi, T. Malik, Optimal control in epidemiology, *Annals of Operations Research*, **251** (2017), 55-71.
[61] C. Sohrabi, Z. Alsafi, N. O'Neill, M. Khan, A. Kerwan, A. Al-Jabir, C. Iosifidis, R. Agha, World Health Organization declares global emergency: A review of the 2019 novel coronavirus (COVID-19), *International Journal of Surgery*, **76** (2020), 71-76.
[62] R. Tandon, COVID-19 and mental health: Preserving humanity, maintaining sanity, and promoting health, *Asian J Psychiatr*, **51** (2020), 102256.
[63] S. Ullah, M. A. Khan, Modeling the impact of non-pharmaceutical interventions on the dynamics of novel coronavirus with optimal control analysis with a case study, *Chaos, Solitons and Fractals*, **139** (2020), 110075.
[64] T. Usherwood, Z. LaJoie, V. Srivastava, A model and predictions for COVID-19 considering population behavior and vaccination, *Scientific Reports*, **11** (2021), 12051.
[65] N. Vindegaard, M. Benros, COVID-19 pandemic and mental health consequences: Systematic review of the current evidence, *Brain, Behavior, and Immunity*, **89** (2020), 531-542.
[66] R. Vinter, *Optimal Control*, Modern Birkäuser Classics, Birkäuser, 2010.
[67] A. Wächter, L. Biegler, On the implementation of a primal-dual interior point filter line search algorithm for large-scale nonlinear programming, *Mathematical Programming*, **106** (2006), 25-57.
[68] W. Wang, J. Tang, F. Wei, Updated understanding of the outbreak of 2019 novel coronavirus (2019-nCoV) in Wuhan, China, *Journal of Medical Virology*, **92** (2020), 441-447.
[69] A. Yousefpour, H. Jahanshahi, S. Bekiros, Optimal policies for control of the novel coronavirus disease (COVID-19) outbreak, *Chaos, Solitons and Fractals*, **136** (2020), 109883.

Received xxxx 20xx; revised xxxx 20xx; early access xxxx 20xx.